ITU – Telecommunications Standardization Sector **Document: Q15-F-21**
STUDY GROUP 16
Video Coding Experts Group (Question 15)

Seoul, Korea, 3–6, November 1998

Question: Q. 15/16
Source: Purdue University, IN., U.S.A. and LG Electronics Inc. Seoul, Korea
Dong Sik Kim, Ness B. Shroff, Jeong Yeol Kim, and Young-Man Park
Tel: +1 765 494 0636, Fax: +1 765 494 3358, Email: dskim@ecn.purdue.edu
Title: **An Adaptive Quantizer Scheme Using Non-Zero Level Codebooks**
Purpose: Proposal

I Introduction

To obtain gains over the quantizer part of the current standards, it is necessary to use *vector quantizers* (VQ) instead of scalar quantizer, i.e., VQ can achieve a gain which cannot be achievable through the scalar quantizer. However, the major disadvantage of VQ is the encoding complexity which increases dramatically as the vector dimension or bit rate increases. The current video coding standard systems are based on high bit-rate quantizers, even when the coding systems are designed for a low bit rate transmission environment. Hence, applying VQ to the current video coding structure is very difficult.

In this proposal, we propose an *adaptive quantizer scheme* (AQS) by employing a feed-forward adaptive quantizer, called *sample-adaptive product quantizer* (SAPQ) (that has recently proposed in [13] and [14]), for the INTER block quantization part of the ITU-T H.263 version 2 (H.263+). Since the structure of this quantizer is based on scalar quantizers, we can readily apply SAPQ to the current quantizer schemes of the video standards. What is remarkable about SAPQ is that it can be used to obtain VQ-level performance with scalar quantization level complexity.

This proposal is organized as follows. In Section II, we concisely describe the uniform SAPQ in preparation for the SAPQ. We introduce the proposed AQS for H.263+, the low bit-rate video coding, in Section III. In Section IV, the design of SAPQ to the INTER block quantization in H.263+ is shown, and simulation results with discussions are given. We then summarize and conclude the proposal in the last section.

II Uniform Sample-Adaptive Product Quantization

In this section, the SAPQ scheme is summarized. We will later demonstrate how to use this scheme in order to quantize the DCT coefficients of H.263+ using non-zero level quantizers.

We consider the random variables $X_1, \cdots, X_m$ as the discrete-time input to be quantized, where m is the *adaptation period* or *sample size*. Suppose that $E\{X_i^2\} < \infty$, for $i = 1, \cdots, m$. Let $\mathcal{C}_n$ denote the class of sets that have n points from $\mathbb{R}$ and let the sets in $\mathcal{C}_n$ be called the n-level codebooks, where each codebook has n codewords. The quantization of X_i is the mapping of a sequence of observations of X_i to a sequence of points of codebook C ($\in \mathcal{C}_n$) according to a map, which is called the quantizer. The average distortion achieved when a random variable X_i is quantized by a codebook C, is given by

$$E\left\{\min_{y \in C}(X_i - y)^2\right\}. \tag{1}$$

In this quantization, the required bit rate R (defined as bits per source symbol) is $R = \log_2 n$ if $C \in \mathcal{C}_n$ and fixed length binary codes are used to represent the quantizer outputs. Note that, since $X_i \in \mathbb{R}$ and $C \subset \mathbb{R}$, the quantizer in (1) is called the *scalar quantizer*.

A. Sample-Adaptive Product Quantizer

Let an observation (or instantiation) of $X_1, \cdots, X_m$ be denoted by $x_1, \cdots, x_m$. We call this observation $x_1, \cdots, x_m$ a *sample*. If we quantize this sample by applying the scalar quantizers using codebooks C_i to each x_i independently, then the overall average distortion is given by

$$D_{\mathrm{PQ}}(R) := E\left\{\frac{1}{m}\sum_{i=1}^{m}\min_{y \in C_i}(X_i - y)^2\right\}. \tag{2}$$

We call this quantization scheme the *product quantizer* (PQ), since the quantizer is a map from $\mathbb{R}^m$ to the product set $\mathbf{C} := \times_{i=1}^{m} C_i = C_1 \times \cdots \times C_m$. Suppose that $C_i \in \mathcal{C}_{n_i}$, then the size of the product set or codebook $\mathbf{C}$ is given by $n = |\mathbf{C}| = \prod_{i=1}^{m} n_i$. Hence, the total bit rate is given by

$$R = \frac{1}{m}\log_2 n = \frac{1}{m}(\log_2 n_1 + \cdots + \log_2 n_m) \tag{3}$$

If the random variables are independent (or uncorrelated), then the independence appears to justify quantizing each random variable independently as shown in PQ of (2). However, even if the input is independent, independently quantizing each random variables $X_1, \cdots, X_m$ is just one of the many possible coding schemes and could be improved from the *block source coding theorem* [2]. If $\mathbf{C}$ is a subset of $\mathbb{R}^m$ with $|\mathbf{C}| = n$, then the average distortion yielded by the VQ for $X_1, \cdots, X_m$ is

$$D_{\mathrm{VQ}}(R) := E\left\{\min_{\mathbf{y} \in \mathbf{C}}\frac{1}{m}\sum_{i=1}^{m}(X_i - y_i)^2\right\}, \tag{4}$$

where $\mathbf{y} = (y_1, \cdots, y_m)$ $(\in \mathbb{R}^m)$ and the bit rate is $R = m^{-1} \log_2 n$.

Now, we introduce the feed-forward adaptive quantization scheme, SAPQ, which is based on a new concept of adaptation to each sample of $X_1, \cdots, X_m$, called *sample adaptation*, in order to improve upon the distortion in (2) [14]. Let $C_{i,j}$ $(\subset \mathbb{R})$ denote the ith codebook for each X_i, where $j \in \{1, 2, \cdots, 2^\eta\}$ and $\eta \in \mathbb{N}$. The adaptive scheme quantizes each sample $x_1, \cdots, x_m$ using the codebooks $C_{1,j}, \cdots, C_{m,j}$ to form the 2^η candidates of distances

$$\frac{1}{m} \sum_{i=1}^{m} \min_{y \in C_{i,j}} (x_i - y)^2, \; j = 1, 2, \cdots, 2^\eta, \tag{5}$$

and then chooses the smallest distance. Hence, SAPQ has the following average distortion:

$$D_{\text{SAPQ}}(R) := E\left\{ \min_{j \in \{1,2,\cdots,2^\eta\}} \frac{1}{m} \sum_{i=1}^{m} \min_{y \in C_{i,j}} (X_i - y)^2 \right\}. \tag{6}$$

Here, let $C_{i,j} \in \mathcal{C}_{n_i'}$. For each sample, the adaptive scheme produces the bit streams for a codebook index and the m quantized element indices, in the form of a feed-forward adaptive coding scheme. This makes it possible to replace different codebooks for each sample of $X_1, \cdots, X_m$. Therefore the total bit rate is given by

$$R = \frac{1}{m}(\log_2 n_1' + \cdots + \log_2 n_m') + \frac{\eta}{m}, \tag{7}$$

where η are the additional bits required in our scheme as side information to indicate which codebook is employed. We call η/m, in (7), the *side bit rate*. Note that we will assume that $\log_2 n_i$ and $\log_2 n_i'$ can be non-integer for performance comparisons. We can consider k-dimensional random vectors as an input of SAPQ. This generalization of SAPQ was studied by us in [13]. SAPQ is a *structurally constrained VQ in m-dimensions* (or km-dimensions in the generalized SAPQ). Hence, we note that SAPQ can achieve the performance of a VQ with dimension less than or equal to m, while maintaining a scalar quantization structure. In fact the encoding complexity of the SAPQ is of the order of a scalar quantizer [13, Appendix B].

It is important to note that SAPQ has a relatively short adaptation period and is very different from the traditional adaptive coding schemes that produce increased gains by replacing the quantizer depending on the varying statistical characteristics of a non-stationary or correlated source [1],[9].

B. Uniform-SAPQ Based on Lattices

In this section, we will study the uniform SAPQs based on several lattices in preparation for the design of the SAPQ codebook for the proposed AQS. If we employ the entropy coder for the outputs of a quantizer, then it is known that using a uniform VQ, such as the lattice VQ, can achieve the performance that is very close to Shannon's theoretical bound. Note that, in this proposal, the SAPQ that is to be employed in the proposed AQS already has the fundamental idea of the lattice VQ, i.e., exploiting the *space-filling advantage*. Hence, we now demonstrate several SAPQs that can implement several important lattice VQs. These examples will be used as a guideline for designing the SAPQ codebooks in the following sections.

In order to study the performance of the uniform SAPQs based on lattices, we will consider a uniformly distributed input as follows. Suppose that $X_1, \cdots, X_m$ are i.i.d. and X_i has a uniform distribution. In other words, we suppose that $\mathbf{X} = (X_1, \cdots, X_m)$ has a uniform density function f given by

$$f(\mathbf{x}) = \begin{cases} 1/a^m, & \mathbf{x} \in \times_{i=1}^{m}[-a/2, a/2] \\ 0, & \text{otherwise}, \end{cases} \tag{8}$$

where a is a positive constant. Note that, for this uniform density function, the gain comes only from the space-filling advantage. Hence, using synthetic data that is uniformly distributed we can numerically observe the achievable gain from the SAPQ by changing the shape of the Voronoi region.

If we use the same m Lloyd-Max (minimum MSE) scalar quantizers for the quantization of $\mathbf{X}$ based on the product quantizer in (2), then the Lloyd-Max quantizer is the uniform quantizer given by output points

$$-\frac{1}{2}(a+b) + b \cdot \ell, \text{ for } \ell = 1, 2, \cdots, n, \tag{9}$$

where $b = a/n$ is the step size. Hence, the average distortion in (2) can be rewritten as

$$D_{\text{PQ}}(R) = \sigma^2 2^{-2R}, \tag{10}$$

where $\sigma^2 = a^2/12$ is the variance of X_i with bit rate $R = \log_2 n$. Note that Shannon's lower bound (SLB) for the uniform density input is less than $D_{\text{PQ}}(R)$ of (10) by $10\log(\pi e/6) = 1.5329\cdots$ dB [14]. Hence, there is a potential of about 1.53 dB improvement, which is the same as the gain $10\log(J_1/\inf J_m)$ from the space-filling advantage.

Let $C_{i,j} := \{y_{1,i,j}, \cdots, y_{n,i,j}\}$ $(\in \mathcal{C}_n)$, for $i = 1, \cdots, m$ and $j = 1, \cdots, 2^\eta$, denote the codebooks of an SAPQ (see (6) for the SAPQ codebooks), where n is a constant such that $\log_2 n \in \mathbb{N}$. Let the codewords be defined as

$$y_{\ell,i,j} := -\frac{1}{2}(a + \frac{3b}{2}) + b \cdot \ell + b_{i,j}, \quad \text{for all } \ell,\ i, \text{ and } j, \tag{11}$$

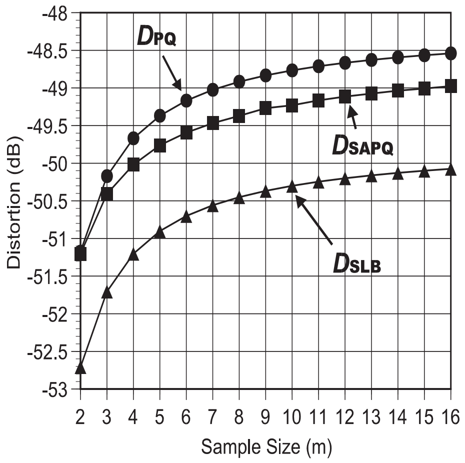

Figure 1: Lattice $D_m^\perp$ based uniform SAPQ ($\eta = 1$) distortion (dB) with respect to the sample size m. ($D_{\rm SLB}$ is Shannon's low bound given by $(6/\pi e)2^{-2R}$.)

where $b = a/n$, $b_{i,j} := rb'_{i,j}$, and $r'_{i,j}$ are given by the *coset representatives* (CRs) $\mathbf{r}'_j := (r'_{1,j}, \cdots, r'_{m,j})(\in \mathbb{R}^m)$ of a lattice. Using this notation, the SAPQ distortion in (6) can be rewritten as

$$D_{\rm SAPQ}(R) = E\left\{ \min_{j\in\{1,\cdots,2^\eta\}} \frac{1}{m} \sum_{i=1}^{m} \min_{\ell\in\{1,\cdots,n\}} (X_i - y_{\ell,i,j})^2 \right\}. \tag{12}$$

From [14, Example 1], for the implementation of an SAPQ based on the lattice $D_m^\perp$, the CRs are given by

$$\text{CR-}D_m^\perp\text{:} \quad \mathbf{r}'_1 = (0, \cdots, 0) \quad \text{and} \quad \mathbf{r}'_2 = 1/2(1, \cdots, 1), \tag{13}$$

for integers m (≥ 2), and $\eta = 1$. (Note that the side bit rate is $\eta/m = 2/m$ bpp, and the SAPQ has two different codebooks.) A block diagram of this quantizer is illustrated in [14, Fig.1]. We now observe the performance of the uniform SAPQ that is designed based on lattice $D_m^\perp$ in (13) for different m. It is known that, for the fixed $\eta = 1$ case, the maximum gain at $m = 9$ is 0.475 dB over the scalar quantizer case in (10) [8],[14]. Further, as m increases above 9, the gain is reduced[1]. In order to verify this fact by experiment, numerical results are illustrated in Fig. 1 for the uniform pdf of (8) with variance 1. In this figure, the bit rate is $R = 8 + 1/m$. However, we can notice a difference in the numerical results in Fig. 1. As m increases from 2, the gain increases and we have a 0.45 dB gain at $m = 8$. However, at $m = 9$, the gain is slightly reduced to 0.43 dB, and then at $m = 10$, achieves the maximum gain of 0.46 dB. As m increases from 10, the gains are monotonically reduced. For example, the gain is 0.39 dB at $m = 32$.

For $m = 8$, the gain from the codebooks of (13) is about 0.475 dB. However, if we set $\eta = 4$ and use the lattice E_8, then we can obtain more gain. For the implementation of the lattice E_8,

[1]The gain in dB is defined as $10\log[D_{\rm PQ}(R)/D_{\rm SAPQ}(R)]$.

the CRs are given by

$$\text{CR-}E_8\text{:}\quad \begin{array}{ll} \mathbf{r}'_1 \;= (0,0,0,0,0,0,0,0), & \mathbf{r}'_2 \;= 1/2(1,1,1,0,1,0,0,0), \\ \mathbf{r}'_3 \;= 1/2(0,1,1,1,0,1,0,0), & \mathbf{r}'_4 \;= 1/2(1,0,0,1,1,1,0,0), \\ \mathbf{r}'_5 \;= 1/2(0,0,1,1,1,0,1,0), & \mathbf{r}'_6 \;= 1/2(1,1,0,1,0,0,1,0), \\ \mathbf{r}'_7 \;= 1/2(0,1,0,0,1,1,1,0), & \mathbf{r}'_8 \;= 1/2(1,0,1,0,0,1,1,0), \\ \mathbf{r}'_9 \;= 1/2(1,1,1,1,1,1,1,1), & \mathbf{r}'_{10} = 1/2(0,0,0,1,0,1,1,1), \\ \mathbf{r}'_{11} = 1/2(1,0,0,0,1,0,1,1), & \mathbf{r}'_{12} = 1/2(0,1,1,0,0,0,1,1), \\ \mathbf{r}'_{13} = 1/2(1,1,0,0,0,1,0,1), & \mathbf{r}'_{14} = 1/2(0,0,1,0,1,1,0,1), \\ \mathbf{r}'_{15} = 1/2(1,0,1,1,0,0,0,1), & \mathbf{r}'_{16} = 1/2(0,1,0,1,1,0,0,1), \end{array} \tag{14}$$

and $\eta = 4$, where $m = 8$ [14, Example 2]. (Note that the side bit rate is $\eta/m = 0.5$ bpp.) The expected gain from the quantizer using CRs given by (14) is approximately 0.654 dB. (A numerical result shows 0.65 dB gain at $n = 256$ [14].) For $m = 8$, when $\eta = 1$, we can design the codebooks of SAPQ based on the lattice $D_m^{\perp}$ as in (13), and when $\eta = 4$, we can design the codebooks based on the lattice E_8 as in (14)[2].

Based on these two lattices, we now design the SAPQ codebooks for $\eta = 2$ and 3, and illustrate the numerical results. For $\eta = 2$, we can choose 4 different CRs from (14). The bit rate is $R = 8.25$ bpp. We consider the following two examples in choosing four CRs,

$$\text{CR-1:}\quad \begin{array}{ll} \mathbf{r}'_1 = (0,0,0,0,0,0,0,0), & \mathbf{r}'_2 = 1/2(1,1,1,1,1,1,1,1), \\ \mathbf{r}'_3 = 1/2(1,0,0,1,1,1,0,0), & \mathbf{r}'_4 = 1/2(0,1,1,0,0,0,1,1) \end{array} \tag{15}$$

and

$$\text{CR-2:}\quad \begin{array}{ll} \mathbf{r}'_1 = (0,0,0,0,0,0,0,0), & \mathbf{r}'_2 = 1/2(0,1,1,1,0,1,0,0), \\ \mathbf{r}'_3 = 1/2(0,0,1,1,1,0,1,0), & \mathbf{r}'_4 = 1/2(0,1,0,0,1,1,1,0). \end{array} \tag{16}$$

However, the two examples show different gains, which are calculated by experiment. CR-1 shows 0.36 dB gain, but CR-2 only shows 0.16 dB gain. We can consider different combinations of the CRs outside the CRs of (14). However, it seems that the best case is CR-1 for $\eta = 2$. (Note that the gain is less than that of the $\eta = 1$ case of (13). This implies that increasing the side bit rate does not always guarantee a better gain.) In a similar manner, we study the $\eta = 3$ case ($R = 8.375$ bpp), where we have 8 different CRs. From the CRs in (14), consider the following 8 CRs,

$$\text{CR-3:}\quad \begin{array}{ll} \mathbf{r}'_1 = (0,0,0,0,0,0,0,0), & \mathbf{r}'_2 = 1/2(1,1,1,1,1,1,1,1), \\ \mathbf{r}'_3 = 1/2(1,1,1,0,1,0,0,0), & \mathbf{r}'_4 = 1/2(0,0,0,1,0,1,1,1), \\ \mathbf{r}'_5 = 1/2(0,1,1,1,0,1,0,0), & \mathbf{r}'_6 = 1/2(1,0,0,0,1,0,1,1), \\ \mathbf{r}'_7 = 1/2(1,0,0,1,1,1,0,0), & \mathbf{r}'_8 = 1/2(0,1,1,0,0,0,1,1). \end{array} \tag{17}$$

[2]Note that the E_8 lattice is the best lattice among the known lattices for the dimension $m = 8$ [7].

The SAPQ using CR-3 produces a 0.40 dB gain. However, if we consider $\mathbf{r}'_1, \mathbf{r}'_2, \cdots, \mathbf{r}'_8$ of CR-E_8 for the 8 CRs, then the gain is 0.34 dB. It seems that the $\eta = 3$ case also yields a lesser gain than the $\eta = 1$ case, even though the number of possible choices (codebooks) is higher than the $\eta = 1$ case.

III Adaptive Quantizer Scheme for H.263+

In this section, we now propose an AQS, which adaptively employs the new quantizer, SAPQ, only for the DCT blocks that require large number of bits.

The optional "alternative INTER VLC" mode of H.263+ [11, Annex S] can improve the coding performance of the quantizer output when significant changes are evident in the picture. In the "busy" INTER blocks, which have a large number of large-magnitude coefficient, the option employs the INTRA VLC table [11, TABLE I.2] of the advanced INTRA coding mode [11, Annex I]. Hence, we can reduce the required bits for the block and maintain the same picture quality. In this proposal, we propose an AQS for such busy blocks in order to reduce the quantizer distortion. In the busy blocks, we use non-zero level quantizers (quantizers that have no zero-value reconstruction level) to obtain gains based on the SAPQ theory. The proposed AQS can be applied to the current option, alternative INTER VLC mode. It is also possible to make further extensions of the application to the quantizers of H.263++.

In the proposed AQS, each block is first classified into two classes: *non-busy block* class and *busy block* class, based on the DCT coefficients of each block. An SAPQ is then applied to the busy blocks only to reduce the distortions of the busy blocks. Non-busy block uses the original quantizer. In the busy blocks, the SAPQ uses several non-zero level quantizers, where only the reconstruction levels are different from the original quantizers of H.263+.

We can consider the following two different methods of classification for finding the busy blocks:

1. Counting the required bits for a block and classifying by using the number of bits by setting a threshold TH for this number.

2. In the alternative INTER VLC mode [11, Annex S], the blocks that use the INTRA VLC table are classified as the busy block.

Note that both these methods do not need any side information to indicate whether the current block is the busy block or not. However, by using the "quantizer information (DQUANT)", we could arbitrary indicate the busy blocks (and then use side information). The first method is a simple classifier without changing the VLC bit stream for the coefficients. If we consider the second method, then the proposed scheme can be applied to the option alternative INTER VLC mode as a modified form of the option. The current option is focussed on reducing the number of required bits. However, if this option is modified by using the AQS, then we can improve the SNR of the busy blocks by reducing the required bits.

We now introduce the quantizer part of the proposed AQS. In a DCT block, we additionally define the following:

QP := quantization parameter,
COF_i := a transform coefficient to be quantized,
$LEVEL_i$:= the quantized version of the transform coefficient, and
REC_i := reconstructed coefficient value,

where i ($\in \{1, \cdots, 64\}$) is the index for the 64 DCT coefficients. We use the following quantization rule, which yields $LEVEL_i$ for the VLC of the INTER coefficients;

$$LEVEL_i = \mathrm{sign}(COF_i) \cdot LEVEL_i', \tag{18}$$

where $LEVEL_i' = \lfloor (|COF_i| - \lfloor QP/2 \rfloor)/(2 \cdot QP) \rfloor$. In order to describe the inverse quantization rule, following inverse quantizers are defined. The first inverse quantization rule, which is designated by IQ_0, is used for the non-busy blocks.

$$\mathrm{IQ}_0 : \; REC_i = \begin{cases} 0, & LEVEL_i = 0 \\ \mathrm{sign}(LEVEL_i) \cdot REC_i', & \text{otherwise}, \end{cases} \tag{19}$$

for $i = 1, \cdots, 64$, where

$$REC_i' = QP \cdot (2 \cdot |LEVEL_i| + 1) - p, \tag{20}$$

and $p = 0$ if QP is odd and $p = 1$ otherwise. (Note that IQ_0 is the same as the original inverse quantization rule for the INTER coefficients in [11]). The recommendation of H.263+ specifies only this inverse quantization rule [11, p.41].) The next set of rules that describe the SAPQs that are used for the the busy blocks in the proposed AQS. For $j = 1, 2, \cdots, 2^\eta$,

$$\mathrm{IQ}_j : \; REC_{i,j} = \begin{cases} c_{i,j}, & LEVEL_i = 0 \\ \mathrm{sign}(LEVEL_i) \cdot REC_i' + d_{i,j}, & \text{otherwise}, \end{cases} \tag{21}$$

for $i = 1, \cdots, 64$, where

$$REC_i' = QP \cdot (2 \cdot |LEVEL_i| + 1) + b_{i,j} - p, \tag{22}$$

and $p = 0$ if QP is odd and $p = 1$ otherwise. In the inverse quantizer IQ_j, $b_{i,j}$, $c_{i,j}$, and $d_{i,j}$ are integers, and j (η bits) is the side information. (Note that these parameters are dependent on i, the index for the DCT coefficient in a DCT block, and $|b_{i,j}|$ and $|c_{i,j}|$ should be even and $|d_{i,j}|$ should be odd to ensure the odd values of REC_i [11].) The design of the parameters and the discussion is introduced in Section IV.

We now introduce the SAPQ quantization rule. Let D_j denote the distance for a busy block that is inversely quantized by IQ_j, where $D_j := 64^{-1}\sum_{i=1}^{64}(COF_i - REC_{i,j})^2$, for $j = 1, 2, \cdots, 2^\eta$. The SAPQ is performed by finding the quantizer that yields the minimum distance among all D_j. From (5), the smallest distance can be rewritten as

$$\min_{j\in\{1,2,\cdots,2^\eta\}} \frac{1}{64}\sum_{i=1}^{64}(COF_i - REC_{i,j})^2. \tag{23}$$

The average of the distances of (23) represents the performance of the proposed AQS. The side information, which has a fixed length η bits, is added to the bit stream of the busy block after the last coefficient so that the bits are decodable.

IV Quantizer Design and Simulation

Designing an SAPQ quantizer in the proposed AQS of (21) is finding the appropriate parameters $b_{i,j}$, $c_{i,j}$, and $d_{i,j}$. In this section, we introduce several designed quantizers and their numerical performance. The simulation was conducted based on the UBC TMN8 [12].

A. Classification

In this proposal, we use the first classification method that is addressed in Section III. First, quantize COF_i according to (18), and using the VLC tables for the INTER blocks [11, TABLES 16,17] and $LEVEL_i$, encode the quantizer output to a bit stream. Next, for each block, count the total bits required for the DCT coefficients (TCOFF) [11]. Note that, if $LEVEL_i = 0$ for all i in a block, then using the "coded macroblock indication" (COD), the "macroblock type and coded block pattern for chrominance" (MCBPC), and the "coded block pattern for luminance" (CBPY) bits, no further information is transmitted for the block. If for some i, $LEVEL_i \neq 0$ in a block, then this block is called a *coded block*. In Fig. 2, the number of coded blocks in each frame of a QCIF (quarter common intermediate format) video sequence, FOREMAN, is illustrated for the 100 frames that were coded as P-pictures. In this figure, $TH = 10$ and $TH = 20$ imply that the number of the coded blocks of the luminance blocks, which is called busy Y-blocks, have more

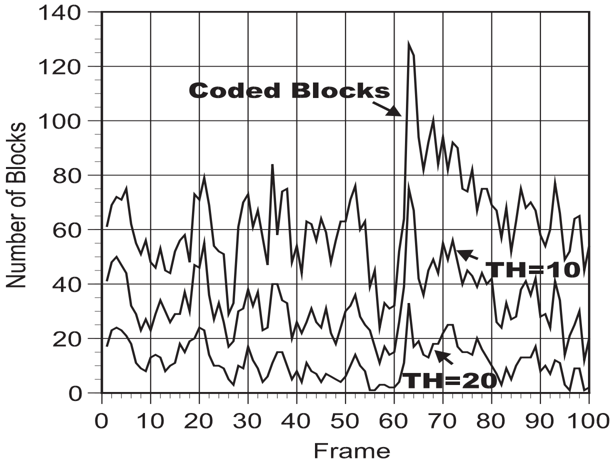

Figure 2: Number of coded blocks in each frame of a QCIF video sequence, FOREMAN at $QP = 16$. ($TH = 10$: Y-blocks that requires more or equal to 10 bits, and $TH = 20$: Y-blocks that requires more or equal to 10 bits.)

or equal to 10 bits and 20 bits for TCOFF, respectively. In the Fig. 2 case, we note that 11 % of the total DCT blocks are coded blocks. (Note that a QCIF frame has 594 DCT blocks.) For an appropriate threshold TH, we classify the luminance blocks into the busy and non-busy Y-blocks. (For example, the blocks that have more than or equal to $TH = 20$ are the busy Y-blocks.) For several values of TH, the peak signal to noise ratios (PSNRs) of the busy Y-blocks are summarized in Table 1, where the signal variance is given by 255^2. Note that the main approach of the proposed AQS is using the SAPQ only for the busy Y-blocks in order to decrease the quantizer distortions of the blocks. Since the chrominance blocks usually require a small number of bits, the expected gain from the SAPQ will be negligible. (Note that the uniform SAPQ obtains a gain from the space-filling advantage.) However, for the chrominance blocks, instead of using SAPQ, simply decreasing QP can obtain good performance in a similar manner to the "modified quantization mode" [11, Annex T].

B. SAPQ Design and Results

The quantizer for the INTER block is a modified uniform quantizer having a dead-zone. Hence, we used different parameters $c_{i,j}$ and $d_{i,j}$ for the zero level and the non-zero level shifting, respectively. Using the CR notation $\mathbf{r}'_j$ ($= (r'_{i,j}, \cdots, r'_{m,j})$) defined after (11), we let

$$c_{i,j} = \begin{cases} DEV_1 \cdot (4 \cdot r'_{i,j} - 1), & \text{for } i = 1, \cdots, m \\ 0, & \text{for } i = m+1, \cdots, 64, \end{cases} \tag{24}$$

for $j = 1, 2, \cdots, 2^\eta$, where a non-negative integer DEV_1 is a shifting constant for the zero level

Table 1: PSNRs (dB) of the busy Y-blocks and the average number of busy blocks per P-picture
FOREMAN QCIF video sequence (100 P pictures by TMN8 at $QP = 16$)
PSNR: Y = 29.81 dB, Cb = 35.30, Cr = 35.74, Average number of bits = 1920 bits/frame
63.4 coded blocks/frame: 27.14 dB

	TH			
	10	20	30	40
PSNR (dB)	26.41	25.69	25.39	25.26
Busy Y-blocks/frame	32.9	11.4	4.9	2.6

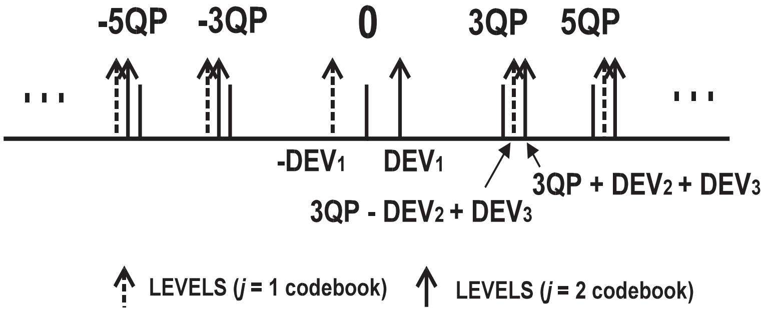

Figure 3: Quantizer reconstruction levels of IQ_j in the SAPQ. (IQ_j for $i = 1, \cdots, m$ in the SAPQ based on CR-$D_m^\perp$.)

in the SAPQ codebooks, and $m \leq 64$. Note that $c_{i,j} \in \{-DEV_1, DEV_1\}$, for $i = 1, \cdots, m$, and $j = 1, 2, \cdots, 2^\eta$. In the same manner, let

$$d_{i,j} = \begin{cases} DEV_2 \cdot (4 \cdot r'_{i,j} - 1), & \text{for } i = 1, \cdots, m \\ 0, & \text{for } i = m+1, \cdots, 64, \end{cases} \tag{25}$$

for $j = 1, 2, \cdots, 2^\eta$, where DEV_2 is a non-negative integer. The parameter $b_{i,j}$ is related to the reconstruction value, which is defined as

$$b_{i,j} = \begin{cases} DEV_3, & \text{for } i = 1, \cdots, m \\ 0, & \text{for } i = m+1, \cdots, 64, \end{cases} \tag{26}$$

where DEV_3 is an integer.

First, we observe the performance of the proposed AQS that is designed based on the lattice $D_m^\perp$. If we consider the lattice $D_m^\perp$, then $\eta = 1$, and $c_{i,j}$ and $d_{i,j}$ are obtained from the two CRs, which are given in (13). The quantizer levels of this SAPQ are illustrated in Fig. 3, where we suppose that $DEV_2 < DEV_3$, and QP is odd. In Fig. 3, the first codebook ($j = 1$) has the negative value $-DEV_1$ instead of the zero level and the second codebook ($j = 2$) has the positive value

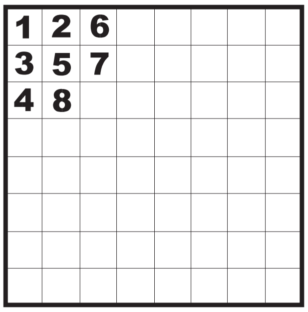

Figure 4: 8×8 DCT block and the 8 coefficients for SAPQ ($m = 8$).

DEV_1 instead of the zero level. Consider only 8 coefficients as shown in Fig. 4, from the 8×8 DCT block. Suppose that the numbers in Fig. 4 are indexed by i. For the other 56 coefficients, we use the inverse quantizer in (18) even when the block is classified into a busy block. In Tables 2 and 3, for $DEV_3 = 4$ and $DEV_3 = 2$, respectively, we provide numerical results of the proposed AQS with respect to DEV_1 and DEV_2. In these simulations, the side bit, η, is added to the next of the last TCOFF so that the decoder can decode the side bit, where the total bits of each frame is aligned with bytes (see TMN8), and the first frame is the I picture with QP and the next 100 frames are P pictures at the same QP. For various values of TH, the results are summarized in Table 4. We note that, for $TH = 10 \sim 40$, the gains are approximately constant around 0.1 dB. These gains increase if we increase the side bits η by employing CR-E_8. For each $D_8^{\perp}$, CR-1, CR-3, and CR-E_8 of section II, the simulation results are summarized in Table 5. From this table, we can also notice the gains for several different video sequences. From Tables 2$\sim$6, we can notice that the overall performance of the AQS and TMN8 are very similar in terms of PSNR and bit rate. However, the AQS shows a better PSNR in the busy Y-blocks. Furthermore, from these tables, we can find that the appropriate values of DEV_1, DEV_2, and DEV_3 for the $QP = 16$ case are $DEV_1 = 7$, $DEV_2 = 2$, and $DEV_3 = 4$.

For different values of the quantization parameter QP, we define the parameters, DEV_1, DEV_2, and DEV_3 as follows.

$$DEV_1 = \lfloor QP/2 \rfloor - p, \tag{27}$$

where $p = 0$ if $\lfloor QP/2 \rfloor$ is odd and $p = 1$ otherwise,

$$DEV_2 = \lfloor QP/8 \rfloor - p, \tag{28}$$

where $p = 0$ if $\lfloor QP/8 \rfloor$ is even and $p = 1$ otherwise, and

$$DEV_3 = \lfloor QP/4 \rfloor - p, \tag{29}$$

where $p = 0$ if $\lfloor QP/4 \rfloor$ is even and $p = 1$ otherwise. The results with respect to QP are shown in Tables 6. We observe that the average bits per frame increase slightly as QP gets small.

C. Subjective Comparison and Non-Zero Level Quantizer

In this section, we compare the performance of the proposed AQS by displaying the reconstructed video sequences. When we compare the reconstructed video sequences, we could consider the following comparison criteria:

1. blocking artifacts between adjacent blocks,
2. smeared/noisy block, and
3. inconstant blocks between frames.

In order to improve the video quality based on these criteria, we should improve all the techniques of the coder, such as motion vector estimation (the loop filter) and the quantizer. In other words, since the blocks in H.263+ are classified into coded and non-coded blocks, i.e., the blocks to be quantized and not quantized, simply increasing the quantizer performance for the busy blocks might result more blocking artifacts especially for large values of the quantization parameter QP. For example, while we compare the two reconstructed video sequences, which are encoded by H.263+ for $QP = 15$ and $QP = 16$, respectively, we could not determine which one was better than the other if we only consider the blocking artifacts. Increasing the quantizer performance is more closely related with the second criterion, "smeared/noisy block". Decreasing QP will obviously reduce the smear and noise inside the block. However, sometimes, decreasing QP enforces several blocks to be quantized, which were non-coded blocks before decreasing QP. Hence the blocks could be noisy blocks due to a marginal quantization between coded and non-coded blocks especially for large QPs. Since the performance of the current frame is dependent on the reference frame, we can observe a similar effect even when QP is fixed if we were to change the quantizer scheme. Even though the block is noisy, however, we can alleviate the smear effect of the block. The noisy blocks could be the main reason for the inconstancy between frames. Therefore, since we only increase the quantizer performance for the busy Y-blocks in the proposed AQS, we focus on the second criterion to compare the reconstructed video sequences.

For the reference video sequences for comparison, we consider two reconstructed video sequences for a given value of QP; TMN8s with QP and $QP - 1$. The same parts of the images from the reconstructed video sequences are illustrated in Figs. 5 and 6 for frame 10 and frame 19, respectively, to show the improvement based on the smear/noise blocks criterion. In these figures,

Table 2: Proposed AQS with respect to the parameters
FOREMAN QCIF video sequence (100 P pictures by TMN8 at $QP = 16$)
CR$-D_8^{\perp}$ $(m = 8)$, $\eta = 1$, $TH = 20$, $DEV_3 = 4$.

Parameters		PSNR (dB)			Busy Y-block	Average
DEV_1	DEV_2	Y	Cb	Cr	PSNR (dB)	bits/frame
7	0	29.84	35.19	35.66	25.88	1909
8	0	29.79	35.34	35.72	25.85	1906
9	0	29.83	35.20	35.63	25.86	1908
7	2	29.84	35.27	35.71	25.89	1908
8	2	29.81	35.24	35.77	25.84	1916
9	2	29.82	35.27	35.65	25.82	1912
TMN8		29.81	35.30	35.74	25.69	1920

Table 3: Proposed AQS with respect to the parameters
FOREMAN QCIF video sequence (100 P pictures by TMN8 at $QP = 16$)
CR$-D_8^{\perp}$ $(m = 8)$, $\eta = 1$, $TH = 20$, $DEV_3 = 2$.

Parameters		PSNR (dB)			Busy Y-block	Average
DEV_1	DEV_2	Y	Cb	Cr	PSNR (dB)	bits/frame
7	0	29.82	35.24	35.73	25.86	1914
8	0	29.81	35.17	35.66	25.82	1915
9	0	29.83	35.30	35.67	25.84	1916
7	2	29.83	35.24	35.69	25.87	1911
8	2	29.83	35.21	35.72	25.80	1925
9	2	29.85	35.30	35.66	25.78	1906
TMN8		29.81	35.30	35.74	25.69	1920

Table 4: Proposed AQS with respect to TH

FOREMAN QCIF video sequence (100 P pictures by TMN8 at $QP = 16$)

CR$-D_8^{\perp}$ ($m = 8$), $\eta = 1$, $DEV_1 = 7$, $DEV_2 = 2$, $DEV_3 = 4$.

TH	PSNR (dB)			Busy Y-block PSNR (dB)		Average
	Y	Cb	Cr	Proposed	TMN8	bits/frame
10	29.83	35.07	35.82	26.51	26.41	1924
20	29.84	35.27	35.71	25.89	25.69	1908
30	29.81	35.30	35.65	25.48	25.39	1902
40	29.83	35.29	35.70	25.36	25.26	1910
TMN8	29.81	35.30	35.74			1920

(a) TMN8 at $QP = 16$: Y=29.81 dB, busy Y-block=25.69 dB, 1920 bits/frame,

(b) TMN8 at $QP = 15$: Y=30.12 dB, busy Y-block=26.11 dB, 2065 bits/frame,

(c) AQS at $QP = 16$ and $\eta = 2$: Y=29.81 dB, busy Y-block=25.69 dB, 1920 bits/frame, $m = 6$ in Fig. 7(a), and

(d) AQS at $QP = 16$ and $\eta = 4$: Y=29.89 dB, busy Y-block=26.21 dB, 1928 bits/frame, $m = 8$ in Fig. 4,

where the PSNRs are obtained for reconstructed 100 P pictures of FOREMAN QCIF video sequences. In Figs. 5 and 6, we observe that (b) has the best quality in the criterion of the smear/noise criterion, i.e., (b) shows the clearest shape among the figures even though there are more blocking artifacts. Focus on his right collar in the figures. In both Figs. 5 and 6, (a) and (c) have a similar blocking artifact and noise in the area. However, (d) shows a similar shape of that of (b). Through the reconstructed video sequences, we can find that the quality of the (d) case is closer to the (b) case than the (a) case. For the $\eta = 2$ case of (c) has a similar quality of that of (a). However, a variation of the case show a better visual quality as shown in Fig. 8(a). The coset representatives CR-1 is modified to

$$\text{CR-1'}: \begin{array}{ll} \mathbf{r}'_1 = (0,0,0,0,0,0), & \mathbf{r}'_2 = 1/2(1,1,1,1,1,1), \\ \mathbf{r}'_3 = 1/2(1,0,0,1,1,1), & \mathbf{r}'_4 = 1/2(0,1,1,0,0,0). \end{array} \tag{30}$$

The TCOFFs for the variation is the 6 coefficients in Fig.7, where $m = 6$. In this numerical result for 100 P pictures, note that the PSNR of the luminance component is 29.84 dB at 1921 bits/frame and the PSNR of the busy Y-blocks is 25.95 dB, which is slightly less than the variation.

We can consider a simple AQS by modifying the TMN8 of QP, where the quantization parameter $QP - 1$ is used for the busy Y-blocks. We can obtain a similar performance of the proposed AQS.

Table 5: Proposed AQS with respect to video sequences and η

QCIF video sequences (100 P pictures by TMN8 at $QP = 16$)

$m = 8$, $DEV_1 = 7$, $DEV_2 = 2$, $DEV_3 = 4$, $TH = 20$

QCIF	AQS	PSNR (dB) Y	PSNR (dB) Cb	PSNR (dB) Cr	Busy Y-block PSNR (dB)	Average bits/frame
FOREMAN	$\eta = 1$ (CR-$D_8^{\perp}$)	29.84	35.27	35.71	25.89	1908
	$\eta = 2$ (CR-1)	29.85	35.27	35.75	25.94	1919
	$\eta = 3$ (CR-3)	29.84	35.19	35.62	25.97	1931
	$\eta = 4$ (CR-E_8)	29.89	35.24	35.61	26.21	1928
	TMN8	29.81	35.30	35.74	25.69	1920
SUZIE	$\eta = 1$ (CR-$D_8^{\perp}$)	32.28	39.48	39.25	27.07	1188
	$\eta = 2$ (CR-1)	32.28	39.41	39.20	27.11	1187
	$\eta = 3$ (CR-3)	32.29	39.42	39.10	27.28	1188
	$\eta = 4$ (CR-E_8)	32.31	39.46	39.17	27.39	1201
	TMN8	32.27	39.49	39.00	26.79	1186
CARPHONE	$\eta = 1$ (CR-$D_8^{\perp}$)	30.84	36.56	36.26	26.23	1323
	$\eta = 2$ (CR-1)	30.83	36.83	36.19	26.38	1332
	$\eta = 3$ (CR-3)	30.85	36.63	36.23	26.47	1327
	$\eta = 4$ (CR-E_8)	30.85	36.75	36.23	26.61	1338
	TMN8	30.82	36.62	36.38	26.16	1315
CLAIRE	$\eta = 1$ (CR-$D_8^{\perp}$)	33.69	35.14	37.80	26.01	431
	$\eta = 2$ (CR-1)	33.70	35.18	37.88	26.13	436
	$\eta = 3$ (CR-3)	33.71	35.13	37.82	26.19	431
	$\eta = 4$ (CR-E_8)	33.70	35.18	37.73	26.18	434
	TMN8	33.70	35.16	37.86	25.72	430

Table 6: Proposed adaptive coding scheme with respect to QP

FOREMAN QCIF video sequence (100 P pictures by TMN8)

CR-1 ($m = 8$), $\eta = 2$, $TH = 20$

QP		PSNR (dB) Y	Cb	Cr	Busy Y-block PSNR (dB)	Average bits/frame
4	AQS	37.00	40.23	41.81	36.61	13511
	TMN8	36.95	40.23	41.82	36.52	13210
8	AQS	33.10	37.53	38.67	30.99	5012
	TMN8	33.06	37.59	38.62	30.86	4916
12	AQS	31.11	36.09	36.94	27.98	2801
	TMN8	31.08	36.07	36.93	27.82	2761
16	AQS	29.85	35.27	35.75	25.94	1919
	TMN8	29.81	35.30	35.74	25.69	1920
20	AQS	28.88	34.68	34.80	24.40	1513
	TMN8	28.86	34.67	34.80	24.17	1492
24	AQS	28.15	34.03	34.21	23.10	1291
	TMN8	28.15	33.97	34.16	22.95	1288
28	AQS	27.62	33.50	33.40	22.09	1154
	TMN8	27.58	33.45	33.56	21.88	1156

(a)

(b)

(c)

(d)

Figure 5: Frame 10 from the reconstructed FOREMAN QCIF video sequence. (a) TMN8 at $QP = 16$. (b) TMN8 at $QP = 15$. (c) AQS at $QP = 16$ and $\eta = 2$. (d) AQS at $QP = 16$ and $\eta = 4$.

(a)

(b)

(c)

(d)

Figure 6: Frame 19 from the reconstructed FOREMAN QCIF video sequence. (a) TMN8 at $QP = 16$. (b) TMN8 at $QP = 15$. (c) AQS at $QP = 16$ and $\eta = 2$. (d) AQS at $QP = 16$ and $\eta = 4$.

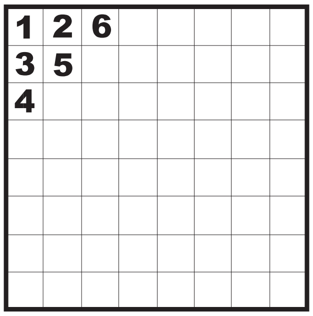

Figure 7: 8×8 DCT block and the 6 coefficients for SAPQ ($m = 6$).

(a) (b)

Figure 8: AQS at $QP = 16$, $\eta = 2$, and $m = 6$. (a) Frame 10. (b) Frame 19.

However, for small quantization parameters, we should increase the bits much higher than the proposed AQS case. We could also combine the SAPQ and the modifed TMN8 scheme.

If we quantize a positive valued signal, then it seems that there is no difference in using the mid-tread or mid-rise type quantizer, where the mid-tread type has the zero level in the output levels, and the mid-rise type does not have the zero level. However, if we consider a quantizer for the DCT coefficients or the residual signals in the differential pulse code modulation (DPCM), then the inputs to be quantized have a high population near zero. (Note that the distributions of these inputs are usually regarded as the Laplacian probability density function [6].) Hence, in this case, it is important to select a quantizer that has the zero level. However, if the distribution of the input is symmetrical and the quantizer output is encoded by fixed binary codes, then the number of levels of the quantizer is a power of 2, i.e., even. Hence, in order to obtain a minimum quantizer distortion, the mid-rise type is usually employed, since the mid-rise type quantizer have an even number of symmetrical levels[3] [3],[4]. However, we might observe *granular noise* on smooth areas especially in the DPCM systems due to the quantizer that does not have the zero level. If we use the entropy coder, such as VLC, for the quantizer outputs, then we can use a mid-tread type quantizer. However, in order to obtain more gain from the run-length coding, the quantizer for the INTER block has the wide quantizer region, called the dead zone. Even though we can reduce the required bits by extending the dead zone, the image quality will be degraded, since a large portion of the input is concentrated around zero, but the quantizer step size is relatively large. Unfortunately, many meaningful non-zero inputs are at the zero level. Using the proposed SAPQ, the non-zero level quantizers, which have small values near zero but have a dead zone in the SAPQ could alleviate this problem.

V Conclusion

In this proposal, for the ITU-T H.263+, we proposed an adaptive quantizer scheme (AQS) by employing the new quantizer scheme, *sample-adaptive product quantizer* (SAPQ). The proposed AQS shows good performance for the range of the quantization parameter QP and different types of the sequences. In the busy blocks, the SNR is increased by $0.1 \sim 0.5$ dB. However, in the overall performance, the proposed AQS has produced the total SNR and bit rate that are equal to or slightly better than in the original scheme. It should be noted that SAPQ can achieve a VQ-level performance at high bit rates with a low encoding complexity of scalar quantizers. Since SAPQ has a scalar quantizer structure, we can easily apply SAPQ to the current coding systems in order to

[3]The quantization in the DCT-based image compression system, which does not employ the entropy coder, is usually based on the mid-rise nonuniform quantizers with a bit allocation technique [5].

obtain a VQ performance as shown in the proposed AQS. Hence, the SAPQ can be combined with any of the current options in H.263+. For example, it is possible to adopt SAPQ in the optional alternative INTER VLC mode (Annex S). Furthermore, we could modify the codebook pattern to obtain a better visual quality.

References

[1] L.R. Rabiner and R.W. Schafer, *Digital Processing of Speech Signals.* New Jersey: Prentice-Hall, 1978.

[2] A.J. Viterbi and J.K. Omura, *Principles of Digital Communication and Coding.* McGraw Hill, 1979.

[3] E.L. Hall, *Computer Image Processing and Recognition*, New York: Academic Press, 1979.

[4] A. Rosenfeld and A.C. Kak, *Digital Picture Processing, vol. 1*, New York: Academic Press, 1982, 2nd. ed.

[5] J.J.Y. Huang and P.M. Schultheiss, "Block quantization of correlated gaussian random variables," *IEEE Trans. Commun. Syst.*, vol. CS-11, pp. 289–296, Sept. 1963.

[6] R.C. Reininger and J.D. Gibson, "Distribution of the two dimensional DCT coefficients for images," *IEEE Trans. Commun.,* vol. COM-31, no.6, pp.835–839, June 1983.

[7] J.H. Conway and N.J.A. Sloane, "On the voronoi regions of certain lattices," *SIAM J. Alg. Discrete Methods,* vol.5, no.3, pp.294–305, Sep. 1984.

[8] J.H. Conway and N.J.A. Sloane, "A lower bound on the average error of vector quantizers," *IEEE Trans. Inform. Theory,* vol. IT-31, no.1, pp.106–109, Jan. 1985.

[9] A. Ortega and M. Vetterli, "Adaptive scalar quantization without side information," *IEEE Trans. Image Processing,* vol. IP-6, no. 5, pp. 665–676, May 1997.

[10] T.R. Gardos, "Video codec test model, near-term, version 8 (TMN8), release 0," ITU-T, Study Group 16, Q15A59, June 1997.

[11] ITU-T, "Video coding for low bit rate communication," ITU-T Recommendation H.263, Jan. 1998.

[12] T.R. Gardos, "Video codec test model, near-term, version 10 (TMN10), draft 1," ITU-T, Study Group 16, Q15D65d1, April 1998.

[13] D.S. Kim and N.B. Shroff, "Sample-adaptive coding scheme (SACS): a structurally constrained vector quantizer," Tech. Rep. TR-ECE 98-14, Purdue University, 1998.

[14] D.S. Kim and N.B. Shroff, "Sample-adaptive product quantization: part I – asymptotic analysis and examples," in preparation, 1998.